Article: Discoveries

Functional evolution of a bark beetle odorant receptor clade detecting monoterpenoids of different ecological origins

Xiao-Qing Hou[1], Jothi Kumar Yuvaraj[1], Rebecca E. Roberts[1], Dan-Dan Zhang[1], C. Rikard Unelius[2], Christer Löfstedt[1], Martin N. Andersson[1]*

[1]Department of Biology, Lund University, Lund, Sweden

[2] Faculty of Health and Life Sciences, Linnaeus University, Kalmar, Sweden

Short title: Functional evolution of odorant receptors

Xiao-Qing Hou, xiaoqing.hou@biol.lu.se

Jothi Kumar Yuvaraj, jothi_kumar.yuvaraj@biol.lu.se

Rebecca Roberts, rebecca.roberts@biol.lu.se

Dan-Dan Zhang, dan-dan.zhang@biol.lu.se

Rikard Unelius, rikard.unelius@lnu.se

Christer Löfstedt, christer.lofstedt@biol.lu.se

Martin N. Andersson, martin_n.andersson@biol.lu.se

*Corresponding author:

Martin N. Andersson, Department of Biology, Sölvegatan 37, 223 62 Lund, Sweden.

Email: martin_n.andersson@biol.lu.se

Phone: +46-(0)462229344

Key words: Functional characterization, Neofunctionalization, Odorant receptor, Olfaction, Purifying selection, *Xenopus* oocyte.

Abstract

Insects detect odors using an array of odorant receptors (ORs), which may expand through gene duplication. How specificities evolve and new functions arise in related ORs within a species remain poorly investigated. We addressed this question by functionally characterizing ORs from the Eurasian spruce bark beetle *Ips typographus*, in which antennal detection and behavioral responses to pheromones, volatiles from host and non-host trees, and fungal symbionts are well described. In contrast, knowledge of OR function is restricted to two receptors detecting the pheromone compounds (*S*)-(–)-ipsenol (ItypOR46) and (*R*)-(–)-ipsdienol (ItypOR49). These receptors belong to a species-specific OR-lineage comprising seven ItypORs. To gain insight into the functional evolution of related ORs, we characterized the five remaining ORs in this clade, using *Xenopus* oocytes. Two receptors responded primarily to the host tree monoterpenes (+)-3-carene (ItypOR25) and *p*-cymene (ItypOR27). Two receptors responded to oxygenated monoterpenoids produced in relatively large amounts by the beetle-associated fungi, with ItypOR23 specific for (+)-*trans*-(1*R*,4*S*)-4-thujanol, and ItypOR29 responding to (+)-isopinocamphone and similar ketones. ItypOR28 responded to the pheromone *E*-myrcenol from the competitor *Ips duplicatus*. Overall, the OR responses match well with those of previously characterized olfactory sensory neuron classes except that neurons detecting *E*-myrcenol have not been identified. The characterized ORs are under strong purifying selection and demonstrate a shared functional property in that they all primarily respond to monoterpenoids. The variation in functional groups among OR ligands and their diverse ecological origins suggest that neofunctionalization has occurred early in the evolution of this OR-lineage following gene duplication.

Introduction

Olfaction is of utmost importance to the ecology of insects, with odors mediating fitness-related activities such as mate choice and the search for food and oviposition sites, and maintenance of symbioses with microbes (Hansson and Stensmyr, 2011; Andersson et al., 2015; Fleischer et al., 2018; Kandasamy et al., 2019). Odors are detected by an expansive gene family encoding odorant receptors (ORs), which are expressed in the olfactory sensory neurons (OSNs) in the insect antennae (Clyne et al., 1999). As such, the ORs are crucial to insect life and they underlie the diverse chemical ecologies, adaptations, niche specializations, and evolutionary divergence seen in the Insecta class, which dominates most habitats of our planet. Yet, the functional evolution of this gene family is poorly understood (but see e.g., Ramdya and Benton, 2010; de

63 Fouchier et al., 2017; Yuvaraj et al., 2017; Guo et al., 2020), and little is known with regards
64 to how new functions evolve in these receptors, especially in non-model insects. This applies
65 to both the molecular mechanics that underlie specificity changes (but see Leary et al., 2012;
66 Hopf et al., 2015) and the ecological selection pressures that drive the evolution of the ORs.

67 New OR genes originate through gene duplication. Hence, the duplicated receptors that are
68 retained and expressed will initially have the same odor specificity as their parental ORs, but
69 may later acquire neutral or adaptive mutations that alter their specificity (Nei et al., 2008;
70 Andersson et al., 2015). One may therefore predict that duplicated "offspring" OR paralogues
71 are likely to adopt similar functions as their "parent" ORs, i.e., detecting compounds with
72 shared chemical characteristics (but see also Adipietro et al., 2012). In this study, we
73 investigated the functional evolution of OR paralogues within a species-specific OR-radiation
74 from the Eurasian spruce bark beetle *Ips typographus* L. (Coleoptera; Curculionidae;
75 Scolytinae).

76 As keystone species in forest ecosystems, bark beetles play an important role in the
77 decomposition of wood and recycling of nutrients (Edmonds and Eglitis, 1989; Raffa et al.,
78 2016). However, a minority of bark beetle species are able to kill healthy trees during outbreak
79 periods, which has become an increasing threat to conifer forests, causing great economic loss
80 (Raffa, 2001; Kausrud et al., 2011; Raffa et al., 2016; Biedermann et al., 2019). In Eurasia, *I.*
81 *typographus* is considered the most serious pest of Norway spruce (*Picea abies*) (Økland and
82 Bjørnstad, 2003). When *I. typographus* population density surpasses a critical threshold, the
83 defense of healthy trees can be overcome through mass-attacks, and entire forest landscapes
84 can be quickly transformed (Wyatt, 2014; Raffa et al., 2016). The mass-attacks are coordinated
85 by a male-produced aggregation pheromone consisting of (4*S*)-*cis*-verbenol and 2-methyl-3-
86 buten-2-ol, attracting both sexes (Schlyter et al., 1987). The attraction is, however, inhibited
87 by several other pheromone compounds produced by *I. typographus* during the later attack
88 phases or by heterospecific beetles, including *E*-myrcenol and specific enantiomers of
89 verbenone, ipsenol, and ipsdienol (Francke et al., 1980: Birgersson et al., 1984; Schlyter et al.,
90 1989; 1992).

91 In addition to the beetle-produced semiochemicals, the pheromone attraction is modulated by
92 volatiles from non-host trees and defense compounds from the host (Zhang and Schlyter, 2004;
93 Andersson et al., 2010; Schiebe et al., 2012; Binyameen et al., 2014; Unelius et al., 2014).
94 Recent laboratory studies have also demonstrated the importance of volatiles in the

95 maintenance of symbioses between *I. typographus* and its fungal associates, with beetle
96 preferences for certain fungi being mediated via olfactory cues (Kandasamy et al., 2019). Once
97 inoculated in a tree, these fungi may provide nutrients to maturing beetles by direct feeding
98 (Kandasamy et al., 2019), metabolize host tree defenses (Kandasamy, 2019), and possibly
99 accelerate tree death (Horntvedt et al., 1983). Extensive efforts have been made to understand
100 the ecological roles of *I. typographus*-associated compounds and to characterize the OSNs that
101 specifically detect them. To date, a total of 23 OSN classes have been reported. The key ligands
102 of these neurons include pheromone compounds from conspecific and heterospecific bark
103 beetles, volatiles from host and non-host plants, and compounds produced by fungal symbionts
104 (Mustaparta et al., 1984; Tømmerås et al., 1984; Tømmerås, 1985; Andersson et al., 2009;
105 Andersson 2012; Raffa et al., 2016; Kandasamy, 2019; Kandasamy et al., 2019; Schiebe et al.,
106 2019; Zhao et al., 2019).

107 The odor selectivity of an OSN depends on the characteristics of the OR that is expressed in
108 that neuron. Hence, functional characterization of ORs is important for understanding the
109 evolution of olfactory specialization. Despite being the largest insect order, functional
110 information of ORs from Coleoptera is, however, limited compared with moths (e.g., Grosse-
111 Wilde et al., 2007; Zhang and Löfstedt, 2015; Zhang et al., 2016; de Fouchier et al., 2017; Guo
112 et al., 2021), flies (e.g., Hallem and Carlson, 2006; Mansourian and Stensmyr, 2015) and
113 mosquitos (Carey et al., 2010; Wang et al., 2010). To our knowledge, only seven beetle ORs
114 have been characterized so far, of which two belong to *I. typographus* (Mitchell et al., 2012;
115 Antony et al., 2020: Mitchell and Andersson 2020; Yuvaraj et al., 2021; Wang et al., 2020). In
116 our previous study, the two *I. typographus* ORs (ItypOR46 and ItypOR49), responded
117 specifically to the pheromone compounds (*S*)-(−)-ipsenol and (*R*)-(−)-ipsdienol respectively.
118 These ORs are part of an *Ips*-specific OR-lineage radiation comprising seven ORs (Yuvaraj et
119 al., 2021). This radiation is present within the coleopteran OR subfamily named Group 7, which
120 is highly expanded in the Curculionidae family (Andersson et al., 2013; Andersson et al., 2019;
121 Mitchell et al., 2020). The other five ORs (ItypOR23, OR25, OR27, OR28 and OR29) in this
122 clade did not respond to any stimulus when tested in HEK293 cells, which was likely due to
123 insufficient protein levels (Yuvaraj et al., 2021). Because this clade represents the largest
124 highly-supported OR-radiation in the antennal transcriptome of this species and many of the
125 OR genes are highly expressed (Yuvaraj et al., 2021), we hypothesize that these ORs have key
126 ecological functions. Thus, targeting the five remaining ORs using a different expression
127 system could provide information on the functional evolution of ORs in this species and also

128 shed light on the general question of how odor specificities may evolve among OR paralogues
129 within species-specific radiations and how their functions relate to species ecology. Hence, the
130 primary aim of this study was to functionally characterize these five ORs using *Xenopus*
131 oocytes and a large panel of ecologically relevant compounds. We asked whether the clade
132 houses additional ORs specifically detecting other bark beetle pheromone compounds, or
133 whether the ORs detect structurally similar chemicals (i.e., oxygenated monoterpenoids) of
134 different biological origins and ecological meanings. The second aim was to link the responses
135 of the functionally characterized ItypORs with the responses of previously identified OSN
136 classes.

137 **Results**

138 *Characteristics of the seven ORs in the* Ips-*specific clade*

139 The five ItypORs targeted for functional characterization are part of an *Ips*-specific OR-lineage
140 comprising seven ItypORs, and this lineage belongs to the monophyletic OR Group 7 in beetles
141 (Mitchell et al., 2020; Yuvaraj et al., 2021). The phylogenetic relationships of these ORs and a
142 subset of additional Group 7 ORs from *I. typographus* and the mountain pine beetle
143 *Dendroctonus ponderosae* ('Dpon') are shown in Fig. 1A. The expression levels (relative to
144 Orco; data from Yuvaraj et al., 2021) and proposed key ligands of the seven ItypORs (based
145 on our oocyte recordings; see below) are shown in Fig. 1B, D. Except for ItypOR27, these OR
146 genes are all among the top 20 (out of 73) most highly expressed OR genes in the antennae of
147 this species (Yuvaraj et al., 2021). The pair-wise amino acid identity amongst the seven ORs
148 ranges from 36.6 % to 49.9 % (Fig. 1C).

149 We evaluated the selective pressure acting on the seven ItypORs by calculating the ratio of
150 nonsynonymous to synonymous substitutions (dN/dS or ω) using PAML (Yang, 1997; Yang
151 and Nielsen, 1998). We first tested whether the clade has a uniform dN/dS ratio (one ratio
152 model, M0) or variable ratios on different branches (free ratio model, M1) by likelihood ratio
153 test (LRT). The result showed that the one ratio model could not be rejected ($P = 0.19$) , and
154 the dN/dS is 0.07623 ($<< 1$) for this clade. We next examined whether there are positively
155 selected sites across the sequences using an LRT, comparing the NSsites models M7 (beta) and
156 M8 (beta and ω). The results showed that the M7 model could not be rejected ($P = 0.93$) , and
157 no positively selected sites were reported across the sequences. Taken together, our dN/dS
158 analysis indicate that the seven ItypORs are under strong purifying selection.

159 *ItypOR23 and ItypOR29 respond to volatiles mainly produced by fungal symbionts*

160 Screening experiments with *Xenopus* oocytes co-expressing ItypOR23 and ItypOrco showed a
161 primary response to (+)-*trans*-4-thujanol, and secondary responses to (±)-3-octanol, (–)-
162 terpinen-4-ol, as well as acetophenone (Fig. 2A and B). Dose-response experiments showed
163 that ItypOR23 is more sensitive to (+)-*trans*-4-thujanol than to the other three compounds (Fig.
164 2C), with this compound eliciting larger responses at each tested concentration. Two recent
165 studies (Schiebe et al., 2019; Kandasamy, 2019) using partly overlapping odor panels
166 characterized an OSN class specific for (+)-*trans*-4-thujanol (named OSN class tMTol), with
167 responses very similar to those of ItypOR23 (Table 1). Although a weak secondary response
168 to 1-octen-3-ol was observed in the OSN (Kandasamy, 2019) but not in the OR, and a weak
169 secondary response to acetophenone in the OR but not in the OSN, the high similarity in the
170 responses to the three best ligands suggests that ItypOR23 is likely to be the matching OR for
171 this OSN class.

172 In the screening experiment, oocytes co-expressing ItypOR29 and ItypOrco responded most
173 strongly to (+)-isopinocamphone, followed by rather strong secondary responses to the
174 structurally similar ketones (+)-pinocamphone, (–)-pinocarvone, (–)-pinocamphone, (–)-
175 isopinocamphone, and (±)-camphor (Fig. 3A and B). As a result of the thermodynamic
176 equilibrium, both the synthesized pinocamphone enantiomers contained 16-19% impurities of
177 the corresponding isopinocamphone enantiomers (Supplementary Table S1), and these may
178 have influenced the responses the pinocamphones. Several additional compounds elicited
179 weaker responses in the screening experiment (Fig. 3B). The dose-response assays confirmed
180 that (+)-isopinocamphone is the primary ligand for this OR, although the responses elicited by
181 the secondary ligands were also comparatively high and similar among the tested compounds
182 (Fig. 3C). The responses of ItypOR29 are highly similar to the responses of the putatively
183 corresponding OSN class (named OSN class Pcn; Schiebe et al., 2019; Kandasamy, 2019),
184 with only minor discrepancies in the rank order among the secondary ligands, which are all
185 similarly active in both systems (Table 1).

186 *ItypOR25 and ItypOR27 respond to host plant volatiles*

187 *Xenopus* oocytes co-expressing ItypOR25 and ItypOrco responded to several compounds in
188 the screening experiment. The strongest response was elicited by the conifer volatile (+)-3-
189 carene followed by the beetle-produced compound (+)-*trans*-verbenol and the non-host plant

190 volatile 1-hexanol. Weaker, yet clear, responses were elicited primarily by lanierone and α-
191 isophorone, whereas responses to additional compounds, such as acetophenone, (±)-3-octanol
192 and (+)-*trans*-4-thujanol, were minor (Fig. 4A and B). The dose-response experiments for
193 ItypOR25 indicated a higher sensitivity to (+)-3-carene as compared to the secondary ligands
194 (Fig. 4C). Previous SSR experiments characterized an OSN class primarily excited by 3-carene
195 (Andersson et al., 2009; Kandasamy, 2019). In addition, several secondary compounds are also
196 shared between this OSN class (named OSN class Δ3; Andersson et al., 2009) and ItypOR25,
197 although the rank orders between them are partially different (Table 1).

198 Oocytes co-expressing ItypOR27 and ItypOrco responded strongly and similarly to the two
199 structurally similar host plant volatiles *p*-cymene and γ-terpinene in the screening assays (Fig.
200 5A and B). A weaker response was elicited by (+)-*trans*-4-thujanol. Dose-response
201 experiments showed that ItypOR27 displayed a slightly higher sensitivity to *p*-cymene than to
202 γ-terpinene, and a lower sensitivity to (+)-*trans*-4-thujanol (Fig. 5C). Similar to this OR, the
203 OSN class originally reported to be highly specific for *p*-cymene (named OSN class pC;
204 Andersson et al., 2009), was recently shown to respond just slightly less to γ-terpinene (Schiebe
205 et al., 2019), and weaker responses to (+)-*trans*-4-thujanol and additional compounds have also
206 been reported (Kandasamy, 2019). Hence, our data for ItypOR27 correspond very well with
207 OSN data reported by Schiebe et al. (2019) (Table 1), whereas several of the weakly activating
208 compounds reported by Kandasamy (2019), were inactive in our oocyte experiments.

209 *ItypOR28 responds to a pheromone component of the sympatric* I. duplicatus

210 Oocytes co-expressing ItypOR28 and ItypOrco were activated by bark beetle pheromones,
211 showing the strongest response to *E*-myrcenol in the screening experiment. *E*-myrcenol is used
212 as an aggregation pheromone component by the competitor *I. duplicatus* (Byers et al., 1990).
213 Secondary responses were elicited by the structurally related compounds ipsdienol and ipsenol
214 (Fig. 6A and B). Dose-response experiments that included *E*-myrcenol, racemic ipsenol,
215 racemic ipsdienol and its two pure enantiomers showed that the response threshold of
216 ItypOR28 is the lowest for *E*-myrcenol, compared with that for both ipsdienol and ipsenol (Fig.
217 6C). An OSN responding to *E*-myrcenol in *I. typographus* has to our knowledge not been
218 reported.

219

220 **Discussion**

221 *Functional evolution of the* I. typographus *OR-radiation*

222 A recent phylogenetic analysis (Yuvaraj et al., 2021) that included the 73 antennally expressed
223 ORs of *I. typographus* along with the ORs from the mountain pine beetle *D. ponderosae*
224 (Andersson et al., 2019) and the Asian longhorn beetle *Anoplophora glabripennis*
225 (Cerambycidae) (McKenna et al., 2016) revealed a highly supported clade formed by seven
226 ItypORs. Two of these receptors (ItypOR46 and ItypOR49) were shown to selectively respond
227 to the pheromone compounds (*S*)-(–)-ipsenol (ItypOR46) and (*R*)-(–)-ipsdienol (ItypOR49)
228 (Yuvaraj et al., 2021). Here, we obtained functional data for the five remaining ItypORs from
229 this clade. Collectively, our results show that this clade contains two ORs specifically tuned to
230 monoterpene hydrocarbons produced by the host tree (ItypOR25 and ItypOR27), three ORs
231 tuned to oxygenated monoterpenoids produced by con- or heterospecific bark beetles (i.e.,
232 pheromone compounds; ItypOR28, ItypOR46, and ItypOR49), and two ORs responding to
233 volatiles produced by the symbiotic fungi of *I. typographus* (ItypOR23 and ItypOR29). Similar
234 to previous suggestions (Mitchell et al., 2012; Mitchell and Andersson 2020; Yuvaraj et al.,
235 2021), these findings strengthen the idea that pheromone receptors from different beetle species
236 do not cluster in specific clades like they tend to do in Lepidoptera where the majority of the
237 characterized pheromone receptors (PRs) are found in the so called classical PR clade (Zhang
238 and Löfstedt, 2015); instead beetle pheromone receptors are scattered in the OR phylogeny,
239 and OR clades include receptors detecting compounds from various ecological sources. This
240 may not be surprising because most bark beetle pheromones are oxygenated monoterpenoids
241 (sometimes produced through metabolism of host monoterpenes) and hence structurally similar
242 to common conifer host tree compounds (and to several fungal-derived compounds),
243 contrasting the situation in moths where most pheromone compounds are structurally different
244 from plant volatiles. In addition, host- and mate localization in bark beetles is an integrated
245 process involving pheromones, host and non-host odors, with aggregation pheromones
246 mediating sex-attraction, aggregation behavior, and successful localization and infestation of
247 host trees providing food.

248 While our functional data suggest a clade in which all ItypORs detect monoterpenes or
249 monoterpenoids and are under strong purifying selection, our findings also bring up questions
250 of how odor specificity may evolve in OR-lineage radiations. Whereas the pheromone
251 compounds ipsenol, ipsdienol, and *E*-myrcenol are similar acyclic monoterpenols with a

252 myrcene backbone, the other ligands for the ORs in this clade include monoterpene
253 hydrocarbons and ketones as well as cyclic structures (Fig. 1D). The splits between the seven
254 ORs appear to be rather old, as indicated by the branch lengths (Fig. 1A) and low amino acid
255 identities (Fig. 1C), and this appears to have provided sufficient time for significant specificity
256 shifts (neofunctionalization) to evolve. Purifying selection against deleterious mutations then
257 appears to have dominated to retain the OR responses to these ecologically important
258 compounds.

259 Previous work (Tømmerås et al., 1984; Andersson et al., 2009) identified OSNs primarily
260 responding to e.g. (*S*)-(+)-ipsdienol and amitinol, which are both structurally related to the
261 primary ligands (*S*)-(–)-ipsenol, (*R*)-(–)-ipsdienol, and *E*-myrcenol of ORs characterized here.
262 Unexpectedly, the ORs detecting these two similar compounds are not found within this
263 receptor lineage, and hence must have evolved their specificities independently. The same
264 holds true for the several OSN classes specifically tuned to monoterpene hydrocarbons or
265 oxygenated monoterpenoids (Andersson et al., 2009; Schiebe et al., 2019; Kandasamy, 2019),
266 of which only four putatively corresponding ORs are localized in this clade.

267 Across several species of Lepidoptera, the structures of key ligands for characterized ORs
268 follow the OR phylogeny at a broader scale, with ligands detected by relatively closely related
269 ORs sharing similar molecular features (de Fouchier et al., 2017; Guo et al., 2021). But similar
270 to our findings, there is also some variation within OR clades with respect to e.g., functional
271 groups and unsaturation among ligands detected by related ORs. For example, the recently
272 identified "novel" PR clade in Lepidoptera harbors receptors responsive to structural isomers
273 of the ligands for the receptors in classical PR clade (Zhang and Löfstedt, 2015), although the
274 two clades are distant (Bastin-Héline et al., 2019). It was suggested that Lepidoptera PRs have
275 evolved independently multiple times, although most of them reside in the classical PR clade.

276 To our knowledge, our study represents a rare example where all ORs in a species-specific OR-
277 radiation comprising as many as seven receptors have been functionally characterized. Hence,
278 large-scale functional characterization of the OR repertoires of *I. typographus* and additional
279 species is required to further our understanding of the functional evolution of the insect OR
280 gene family.

281

282 *ItypOR23 and ItypOR29 detect volatiles mainly produced by fungal symbionts*

283 Like other bark beetles, *I. typographus* is associated with a suite of symbiotic ophiostomatoid
284 fungi, which beetles inoculate into the inner bark of attacked trees. These fungi may serve as
285 food for maturing beetles (Kandasamy et al., 2019) and they also metabolize spruce defense
286 compounds (Kandasamy, 2019). In laboratory bioassays, beetles actively seek out fungal-
287 colonized media using olfactory cues and are able to distinguish different fungal species by
288 their different odor profiles using OSNs dedicated for fungal volatiles (Kandasamy et al., 2019).
289 Here, we characterized two receptors, ItypOR23 and ItypOR29, responding to the fungal-
290 derived volatiles (+)-*trans*-4-thujanol and (+)-isopinocamphone, respectively. Both of these
291 ORs showed high response specificities to only a few structurally related compounds. The OR
292 response profiles matched very well with those from the characterized OSNs, where the tMTol
293 class is highly specific for (+)-*trans*-4-thujanol and the Pcn class selective for the highly similar
294 monoterpene ketones that activate ItypOR29 (Table 1; Schiebe et al., 2019; Kandasamy, 2019).

295 It was recently shown that the fungi of *I. typographus* transform the host compounds (–)-β-
296 pinene, (–)-α-pinene and (–)-bornyl acetate to oxygenated monoterpenoids, including the
297 primary and secondary ligands of both ItypOR23 and ItypOR29 (Kandasamy, 2019). In lab
298 bioassays, (+)-*trans*-4-thujanol and camphor were attractive to adult beetles at a relatively low
299 dose (100 µg), however, (+)-*trans*-4-thujanol was repellent at higher doses (200 µg to 1 mg)
300 (Blažytė-Čereškienė et al., 2016; D. Kandasamy, M. N. Andersson, A. Hammerbacher, J.
301 Gershenzon et al., unpublished data). This suggests concentration-dependent effects of these
302 compounds and that changes in their emission over time may be used by new incoming bark
303 beetles to evaluate the colonization status of the host tree. In addition to production by fungi,
304 these oxygenated monoterpenoids are also released from spruce trees, with amounts decreasing
305 with tree age and increasing with tree stress (Blažytė-Čereškienė et al., 2016; Schiebe et al.,
306 2019). Hence, these compounds of multiple ecological origins may be also used by *I.*
307 *typographus* to assess the physiological status of host trees.

308 *ItypOR25 and ItypOR27 are tuned to host plant volatiles*

309 ItypOR25 and OR27 were most sensitive to two host monoterpenes, (+)-3-carene and *p*-
310 cymene, respectively, and especially ItypOR27 demonstrated a high specificity. These two
311 ORs group together within the analyzed OR clade and present the most recent split among the
312 seven ORs, which is in line with a tuning shift from detecting oxygenated monoterpenoids to

313 monoterpene hydrocarbons. Despite this shared characteristic, the response profiles of the two
314 ORs are widely different suggesting that neofunctionalization has been favored also after their
315 presumed duplication (Rastogi and Liberles, 2005; Andersson et al., 2015). Whereas the
316 response profile of ItypOR27 matches very well with that of the pC OSN class, ItypOR25
317 presented a worse match with a broader response profile and partly different rank orders among
318 the secondary compounds compared to the putatively corresponding Δ3 OSN class (Table 1;
319 Andersson et al., 2009; Schiebe et al., 2019). It remains unknown whether this discrepancy is
320 due to the artificial oocyte environment or whether ItypOR25 is not the receptor of the Δ3 OSN
321 class. However, differences in OR responses between different *in vitro* systems and between
322 these systems and the OSNs have repeatedly been found in previous studies, including for
323 ItypOR46 and ItypOR49 and corresponding OSN classes (Yuvaraj et al., 2017; Yuvaraj et al.,
324 2021; Hou et al., 2020). Because of this system-dependency and since no other OSN in *I.*
325 *typographus* has shown a primary response to 3-carene (Andersson et al., 2009; Schiebe et al.,
326 2019; Kandasamy, 2019; Kandasamy et al., 2019), it appears likely that ItypOR25 is indeed
327 the receptor that corresponds to the Δ3 OSN class.

328 The roles of host monoterpenes in host selection by *I. typographus* is poorly understood and
329 likely context-dependent. While attraction to host monoterpenes alone has not been
330 demonstrated, the major host compounds α-pinene and β-pinene can enhance the response of
331 the bark beetle to the aggregation pheromone (Rudinsky et al., 1972; Hulcr et al., 2006; Erbilgin
332 et al., 2007). In contrast, less abundant host compounds may reduce the pheromone attraction.
333 For example, 1,8-cineole is more abundant in resistant trees and upregulated during an attack,
334 and this compound has a strong antagonistic effect on pheromone attraction (Andersson et al.,
335 2010; Schiebe et al., 2012; Binyameen et al., 2014). Similarly, *p*-cymene is increased in heavily
336 attacked trees, and it reduced pheromone trap catch by 50% (Andersson et al., 2010). Hence,
337 increased amounts of inducible toxic host compounds may be used by bark beetles as cues to
338 evaluate host defense potential and/or breeding density, and may therefore represent general
339 'host unsuitability' signals (Erbilgin and Raffa, 2000; Seybold et al., 2006; Andersson et al.,
340 2010) with context- and species-dependent effects (Saint-Germain et al., 2007; Raffa et al.,
341 2016). To our knowledge, behavioral effects of 3-carene have not been studied in *I.*
342 *typographus.* However, the amount of 3-carene in Norway spruce increases after inoculation
343 with the *I. typographus*-associated fungus *Endoconidiophora polonica*, and this compound has
344 been linked to conifer resistance and susceptibility to insects and fungi (Zhao et al., 2010, and
345 references therein). In addition, 3-carene is also abundant in pine trees, including sympatric

346 Scots pine (*Pinus sylvestris*) and it may hence be used as a host suitability cue, similar to *p*-
347 cymene and 1,8-cineole.

348 *ItypOR28, ItypOR46, and ItypOR49 detect bark beetle pheromones*

349 We characterized one bark beetle pheromone receptor (ItypOR28) primarily responding to *E*-
350 myrcenol. Hence, together with the previously characterized ItypOR46 ((*S*)-(–)-ipsenol) and
351 ItypOR49 ((*R*)-(–)-ipsdienol) (Yuvaraj et al., 2021), the targeted clade houses three pheromone
352 receptors. The ipsenol and ipsdienol enantiomers are produced by male *I. typographus* during
353 the later attack phases (2-6 days after boring has been initiated), and at least ipsenol inhibits
354 the attraction to the aggregation pheromone, possibly to avoid intraspecific competition
355 (Francke et al., 1980; Birgersson et al., 1984; Schlyter et al., 1989). *E*-myrcenol together with
356 both enantiomers of ipsdienol comprise the aggregation pheromone of *I. duplicatus*, the largest
357 competitor of *I. typographus* (Byers et al., 1990), and *E*-myrcenol inhibits the attraction of *I.*
358 *typographus* to its aggregation pheromone (Schlyter et al., 1992). Consistent with a general
359 high specificity of insect pheromone receptors (Andersson et al., 2015), ItypOR28 only
360 responded secondarily to the structurally related ipsdienol and ipsenol, and narrow tunings
361 were also reported for ItypOR46 and ItypOR49 (Yuvaraj et al., 2021). In contrast to the four
362 other ItypORs characterized here, no OSN class has been reported to be specific for *E*-myrcenol
363 despite large screening efforts that included this compound (Andersson et al., 2009). Our
364 results from ItypOR28 suggest the existence of such an OSN class, and it is possible that these
365 OSNs have been missed because some OSN classes were recently shown to have a highly
366 restricted spatial distribution on the *I. typographus* antenna (Kandasamy et al., 2019).

367 *Concluding remarks*

368 We determined the functions of five ORs from a species-specific clade formed by seven
369 receptors in *I. typographus* using the *Xenopus* oocyte system. Together with the two
370 pheromone receptors previously characterized in HEK cells and oocytes (Yuvaraj et al., 2021),
371 this clade contains seven ORs which respond to monoterpenes or monoterpenoids, indicating
372 the biological importance of such compounds to *I. typographus*. Three ORs respond to bark
373 beetle pheromones, two ORs to host plant volatiles, and two ORs to (mainly) fungal-derived
374 compounds. The structural similarities especially among the three pheromonal ligands detected
375 by ItypOR28, ItypOR46, and ItypOR49 implies that the ORs in this species-specific radiation
376 have evolved specificities for chemically similar compounds. In addition, the variation in the

377 structures of the key ligands for the seven receptors and their various ecological origins suggest
378 that neofunctionalization has been promoted in the evolution of this OR clade after which
379 purifying selection has dominated to retain the new OR responses. Finally, our results indicate
380 that the pheromone receptors of beetles do not form specific pheromone receptor clades as seen
381 in Lepidoptera (Yuvaraj et al., 2018). Instead, beetle pheromone receptors are dispersed across
382 the OR phylogeny, and OR-lineage radiations within species contain receptors that detect
383 compounds of different ecological origins.

384 **Materials and methods**

385 *Chemicals*

386 Compounds tested in this study were from commercial sources, synthesized by the Unelius
387 laboratory or obtained from colleagues as gifts (Table S1). The test compounds included beetle-
388 produced pheromone compounds, and volatiles produced by associated fungi, conifer host and
389 angiosperm non-host trees, including the key ligands for all known OSN classes of *I.*
390 *typographus* as well as several secondary ligands for these neurons (Tömmerås, 1985;
391 Andersson et al., 2009; Schiebe et al., 2019; Kandasamy, 2019; Kandasamy et al., 2019). Stock
392 solutions for *Xenopus* oocyte recordings were prepared by diluting each compound to 100 mM
393 in dimethyl sulfoxide (DMSO), which were stored at -20°C. Before each experiment, the stock
394 solutions were diluted to desired concentration in Ringer´s buffer (96 mM NaCl, 2 mM KCl,
395 5mM $MgCl_2$, 0.8 mM $CaCl_2$, 5 mM HEPES, pH 7.6) with the final stimuli containing 0.1%
396 DMSO. Ringer´s buffer containing 0.1% DMSO was used as negative control. Compounds
397 were initially screened for receptor activity at a concentration of 100 µM, and the active
398 compounds were subsequently tested in dose-response experiments using six concentrations at
399 10-fold increments ranging from 1 nM to 100 µM. An odor panel of 32 compounds was initially
400 tested on all five ORs (ItypOR23, 25, 27, 28, and 29) (Table S1). After obtaining the first
401 screening responses to this odor panel, additional OR-specific compounds (putative secondary
402 ligands) were selected for testing based on previous data from putatively matching OSN types,
403 which facilitated our comparisons of OR responses with those of previously characterized OSN
404 classes (Table S2). For consistency, these nine additional compounds were also tested on the
405 other non-target ORs over two replications (showing insignificant activity). For ItypOR28, the
406 initial screening experiment indicated only minor and rather unspecific responses to some test
407 compounds. Hence, we hypothesized that this OR may be tuned to a structurally related
408 compound, and therefore also tested frontalin, *E*-myrcenol and myrtenol specifically on this

409 OR (Table S3). Chemical structures presented in Fig. 1D were drawn using ChemDraw
410 Professional 17.0.

411 *Vector construction and cRNA synthesis*

412 Full length sequences of ItypORs and ItypOrco were amplified by PCR using gene specific
413 primers containing flanking 5' Kozak sequence ('GCCACC') and 5' and 3' recognition sites
414 for restriction enzymes (Table S4). The expression vectors pcDNA5/TO containing the five
415 ItypORs (ItypOR23, 25, 27, 28, and 29; amino acid sequences are available in the
416 Supplementary Material) and pcDNA4/TO containing ItypOrco that were used in previous
417 HEK293 cell assays (Yuvaraj et al., 2021) were used as templates for sub-cloning. Sequences
418 of the five ItypORs have been deposited in GenBank under the accession numbers MW556722-
419 MW556726. The PCR products were analyzed on 1% TAE agarose gels, and then purified
420 using the GeneJET Gel Extraction Kit (Thermo Fisher Scientific™). The purified fragments
421 were ligated into the oocyte expression vector pCS2+ using T4 ligase (Thermo Fisher Scientific)
422 overnight at 4 °C and then transformed into TOP10 competent cells (Thermo Fisher Scientific).
423 Positive colonies that were confirmed by colony PCR were grown in LB broth overnight with
424 ampicillin, and the plasmids were then extracted using the GeneJET plasmid miniprep kit
425 (Thermo Fisher Scientific). Plasmids were Sanger sequenced on a capillary 3130xL Genetic
426 Analyzer (Thermo Fisher Scientific, Waltham, MA, USA) using Sp6 and EBV-rev primers at
427 the sequencing facility at the Department of Biology, Lund University. Large quantities of
428 purified plasmids containing ItypORs and ItypOrco with correct sequences were obtained
429 using the PureLinkTM HiPure Plasmid Filter Midiprep Kit (Thermo Fisher Scientific). cRNAs
430 of ItypORs and ItypOrco were synthesized from NotI (Promega) linearized recombinant
431 pCS2+ plasmids using the mMESSAGE mMACHINE SP6 transcription kit (Thermo Fisher
432 Scientific).

433 *Microinjection and two-electrode voltage clamp recordings*

434 Each of the five ItypORs were co-expressed with ItypOrco in *Xenopus laevis* oocytes, and two-
435 electrode voltage clamp recordings were performed following previously described protocols
436 (Zhang et al., 2010; Zhang and Löfstedt, 2013). In brief, oocytes were surgically collected from
437 *X. laevis* females (frogs were purchased from University of Portsmouth, UK) and treated with
438 1.5 mg/mL collagenase (Sigma-Aldrich Co., St. Louis, MO, USA) in oocyte Ringer 2 buffer
439 (82.5 mM NaCl, 2 mM KCl, 1mM $MgCl_2$, 5mM HEPES, pH 7.5) at room temperature for 15-

440 18 min. Mature healthy oocytes (stage V-VII) were co-injected with 40 ng each of candidate
441 OR and Orco cRNAs, then incubated for 3-7 days at 18 °C in Ringer´s buffer containing
442 sodium pyruvate (550 mg/L) and gentamicin (100 mg/L). Odorant-induced whole-cell inward
443 currents were recorded from injected oocytes in good condition using a two-electrode voltage
444 clamp with a TEC-03BF amplifier at the holding potential of -80 mV. A computer-controlled
445 perfusion system was employed to apply the tested compounds and Ringer´s buffer to the
446 oocyte chamber. Oocytes were exposed to compounds at a flow rate of 2 mL/min for 20 s with
447 extensive washing with Ringer´s buffer at a flow rate of 4 mL/min between stimulations to
448 recover the current to baseline. Data were collected and analyzed using the Cellworks software
449 (NPI Electronic GmbH, Tamm, Germany), and the responses were normalized by calculating
450 the relative response to each active compound in relation to the average response to the most
451 active compound.

452 *Evolutionary analysis of ORs*

453 Amino acid sequences of select Group 7 ORs (Mitchell et al., 2020) from *I. typographus* and
454 *D. ponderosae* were aligned using MAFFT (v7.450; Katoh et al., 2002), and an unrooted
455 maximum likelihood tree was constructed using FastTree 2.1.11 (Price et al., 2010)
456 implemented in Geneious Prime (2020.0.5) software (Biomatters Ltd., Auckland, New
457 Zealand). Local node support values were calculated using the Shimodaira-Hasegawa (SH) test
458 implemented in FastTree. The nonsynonymous (dN) to synonymous (dS) substitution rate (ω)
459 was estimated by the maximum likelihood method (Anisimova et al., 2001) using the Codeml
460 program in the PAML 4.6 package (Yang, 1997).

461 **Acknowledgements**

462 We are grateful to Dineshkumar Kandasamy, Suresh Ganji, Erika Wallin, Blanka Kalinová,
463 Fredrik Schlyter, Anna Jirošová, and Aleš Machara for providing test compounds. We thank
464 the Chinese Scholarship Council (CSC) for finical support of Xiaoqing Hou´s PhD study. This
465 work was also supported by grants from the Swedish Research Councils FORMAS (grants
466 #217-2014-689 and #2018-01444 to M.N.A.) and VR (#2017-03804 to C.L.), the Crafoord
467 foundation (M.N.A.), the Carl Trygger foundation (M.N.A.), and the Royal Physiographic
468 Society in Lund (R.E.R. and M.N.A.). The study was carried out as part of the Max Planck
469 Centre for Next Generation Chemical Ecology (nGICE).

470 **Data availability**

471 All oocyte data are presented in the main figures of the paper. Sequences of the characterized
472 ItypORs have been deposited in Genbank (accession numbers MW556722-MW556726).

473

474 **References**

475 Adipietro KA, Mainland JD, Matsunami H. 2012. Functional evolution of mammalian odorant
476 receptors. *PLoS Genet.* 8:e1002821

477 Andersson MN, Grosse-Wilde E, Keeling CI, Bengtsson JM, Yuen MM, Li M, Hillbur Y,
478 Bohlmann J, Hansson BS, Schlyter F. 2013. Antennal transcriptome analysis of the
479 chemosensory gene families in the tree killing bark beetles, *Ips typographus* and
480 *Dendroctonus ponderosae* (Coleoptera: Curculionidae: Scolytinae). *BMC Genomics*
481 14:198.

482 Andersson MN, Keeling CI, Mitchell RF. 2019. Genomic content of chemosensory genes
483 correlates with host range in wood-boring beetles (*Dendroctonus ponderosae*, *Agrilus*
484 *planipennis*, and *Anoplophora glabripennis*). *BMC Genomics.* 20:690.

485 Andersson MN, Larsson MC, Schlyter F. 2009. Specificity and redundancy in the olfactory
486 system of the bark beetle *Ips typographus*: Single-cell responses to ecologically relevant
487 odors. *J Insect Physiol*. 55(6):556-567.

488 Andersson MN, Larsson MC, Blaženec M, Jakuš R, Zhang QH, Schlyter F. 2010. Peripheral
489 modulation of pheromone response by inhibitory host compound in a beetle. *J Exp Biol.*
490 213:3332-3339.

491 Andersson MN, Löfstedt C, Newcomb RD. 2015. Insect olfaction and the evolution of receptor
492 tuning. *Front Ecol Evol*. 3:53.

493 Andersson MN. 2012. Mechanisms of odor coding in coniferous bark beetles: From neuron to
494 behavior and application. *Psyche J Entomol.* 2012:149572.

495 Anisimova M, Bielawski JP, Yang Z. 2001. Accuracy and power of the likelihood ratio test in
496 detecting adaptive molecular evolution. *Mol Biol Evol*. 18:1585-1592.

497 Antony B, Johny J, Montagné N, Jacquin-Joly E, Capoduro R, Cali K, Persaud K, Al-Saleh MA,
498 Pain A. 2020. Pheromone receptor of the globally invasive quarantine pest of the palm tree,
499 the red palm weevil (*Rhynchophorus ferrugineus*). bioRxiv preprint
500 https://doi.org/10.1101/2020.07.31.230326.

Bastin-Héline L, De Fouchier A, Cao S, Koutroumpa F, Caballero-Vidal G, Robakiewicz S, Monsempes C, François MC, Ribeyre T, Maria A, Chertemps T. 2019. A novel lineage of candidate pheromone receptors for sex communication in moths. *Elife* 8:e49826.

Biedermann PHW, Müller J, Grégoire JC, Gruppe A, Hagge J, Hammerbacher A, et al. 2019. Bark beetle population dynamics in the Anthropocene: challenges and solutions. *Trends Ecol Evol.* 34(10):914-924.

Binyameen M, Jankuvová J, Blaženec M, Jakuš R, Song L, Schlyter F, Andersson MN. 2014. Co-localization of insect olfactory sensory cells improves the discrimination of closely separated odor sources. *Funct Ecol.* 28(5):1216-1223.

Birgersson G, Schlyter F, Löfqvist J, Bergström G. 1984. Quantitative variation of pheromone components in the spruce bark beetle *Ips typographus* from different attack phases. *J Chem Ecol.* 10:1029-1055.

Blažytė-Čereškienė L, Apšegaitė V, Radžiutė S, Mozūraitis R, Būda V, Pečiulytė D. 2016. Electrophysiological and behavioural responses of *Ips typographus* (L.) to *trans*-4-thujanol—a host tree volatile compound. *Ann For Sci.* 73(2):247-256.

Byers JA, Schlyter F, Birgersson G, Francke W. 1990. *E*-myrcenol in *Ips duplicatus*: An aggregation pheromone component new for bark beetles. *Experientia* 46:1209-1211.

Carey AF, Wang G, Su CY, Zwiebel LJ, Carlson JR, 2010. Odorant reception in the malaria mosquito *Anopheles gambiae*. *Nature* 464(7285):66-71.

Clyne PJ, Warr CG, Freeman MR, Lessing D, Kim J, Carlson JR. 1999. A novel family of divergent seven-transmembrane proteins: candidate odorant receptors in *Drosophila*. *Neuron* 22(2):327-338.

de Fouchier A, Walker WB, Montagne N, Steiner C, Binyameen M, Schlyter F et al. 2017. Functional evolution of Lepidoptera olfactory receptors revealed by deorphanization of a moth repertoire. *Nat Commun.* 8:15709.

Edmonds RL, Eglitis A. 1989. The role of the Douglas-fir beetle and wood borers in the decomposition of and nutrient release from Douglas-fir logs. *Can J For Res.* 19(7):853-859.

Erbilgin N, Krokene P, Kvamme T, Christiansen E. 2007. A host monoterpene influences *Ips typographus* (Coleoptera: Curculionidae Scolytinae) responses to its aggregation pheromone. *Agric For Entomol.* 9:135-140.

532 Erbilgin N, Raffa KF. 2000. Opposing effects of host monoterpenes on responses by two
533 sympatric species of bark beetles to their aggregation pheromones. *J Chem Ecol.* 26:2527-
534 2548.

535 Fleischer J, Pregitzer P, Breer H, Krieger J. 2018. Access to the odor world: olfactory receptors
536 and their role for signal transduction in insects. *Cell Mol Life Sci.* 75(3):485-508.

537 Francke W, Sauerwein P, Vité JP, Klimetzek D. 1980. The pheromone bouquet of *Ips amitinus*.
538 *Naturwissenschaften* 67:147-148.

539 Grosse-Wilde E, Gohl T, Bouche E, Breer H, Krieger J. 2007. Candidate pheromone receptors
540 provide the basis for the response of distinct antennal neurons to pheromonal compounds.
541 *Eur J Neurosci.* 25(8):2364-2373.

542 Guo M, Du L, Chen Q, Feng Y, Zhang J, Zhang X, Tian K, Cao S, Huang T, Jacquin-Joly E,
543 Wang G, Liu Y. Odorant receptors for detecting flowering plant cues are functionally
544 conserved across moths and butterflies. *Mol. Biol. Evol.* 2021; 38(4): 1413-1427.

545 Hallem EA, Carlson JR. 2006. Coding of odors by a receptor repertoire. *Cell* 125(1):143-160.

546 Hansson BS, Stensmyr MC. 2011. Evolution of insect olfaction. *Neuron* 72(5):698-711.

547 Hopf TA, Morinaga S, Ihara S, Touhara K, Marks DS, Benton R. 2015. Amino acid coevolution
548 reveals three-dimensional structure and functional domains of insect odorant receptors.
549 *Nat Commun.* 6:6077.

550 Horntvedt R, Christiansen E, Solheim H, Wang S. 1983. Artificial inoculation with *Ips*
551 *typographus*-associated blue stain fungi can kill healthy Norway spruce trees. *Medd Nor*
552 *Inst Skogforsk.* 38:1-20.

553 Hou X, Zhang DD, Yuvaraj JK, Corcoran1 JA, Andersson MN, Löfstedt C. 2020. Functional
554 characterization of odorant receptors from the moth *Eriocrania semipurpurella*: a
555 comparison of results in the *Xenopus* oocyte and HEK cell systems. *Insect Biochem Mol*
556 *Biol.* 117:103289.

557 Hulcr J, Ubik K, Vrkoc J. 2006. The role of semiochemicals in tritrophic interactions between
558 the spruce bark beetle *Ips typographus*, its predators and infested spruce. *J Appl Entomol.*
559 130(5):275-283.

560 Kandasamy D. 2019. Chemical interactions between the spruce bark beetle (*Ips typographus*),
561 its host tree (*Picea abies*), and its fungal associates. PhD Thesis; Friedrich-Schiller-
562 Universität, Fakultät für Biowissenschaften, Jena, Germany.

563 Kandasamy D, Gershenzon J, Andersson MN, Hammerbacher AV. 2019. Volatile organic
564 compounds influence the interaction of the Eurasian spruce bark beetle (*Ips typographus*)
565 with its fungal symbionts. *ISME J.* 13:1788-1800.

566 Katoh K, Misawa K, Kuma Ki, Miyata T. 2002. MAFFT: a novel method for rapid multiple
567 sequence alignment based on fast Fourier transform. *Nucleic Acids Res.* 30(14):3059-3066.

568 Kausrud KL, Grégoire JC, Skarpaas O, Erbilgin N, Gilbert M, Økland B, Stenseth NC. 2011.
569 Trees wanted—dead or alive! Host selection and population dynamics in tree-killing bark
570 beetles. *PLoS ONE.* 6(5):e18274.

571 Leary GP, Allen JE, Bunger PL, Luginbill JB, Linn CE, Macallister IE, Kavanaugh MP,
572 Wanner KW. 2012. Single mutation to a sex pheromone receptor provides adaptive
573 specificity between closely related moth species. *Proc Natl Acad Sci U S A.*
574 109(35):14081-14086.

575 Mansourian S, Stensmyr MC. 2015. The chemical ecology of the fly. *Curr Opin Neurobiol.*
576 34:95-102.

577 McKenna DD, Scully ED, Pauchet Y, Hoover K, Kirsch R, Geib SM, Mitchell RF, Waterhouse,
578 RM, Ahn SJ, Arsala D. et al. 2016. Genome of the Asian longhorned beetle (*Anoplophora*
579 *glabripennis*), a globally significant invasive species, reveals key functional and
580 evolutionary innovations at the beetle–plant interface. *Genome Biol.* 17:227.

581 Mitchell RF, Andersson MN. 2020. Olfactory genomics of the Coleoptera. In: Blomquist GJ,
582 Vogt RG, editors. Insect Pheromone Biochemistry and Molecular Biology 2nd Edition.
583 Academic Press, Oxford. p. 547-590.

584 Mitchell RF, Hughes DT, Luetje CW, Millar JG, Soriano-Agatón F, Hanks LM, Robertson,
585 HM. 2012. Sequencing and characterizing odorant receptors of the cerambycid beetle
586 *Megacyllene caryae*. *Insect Biochem Mol Biol.* 42(7):499-505.

587 Mitchell RF, Schneider TM, Schwartz AM, Andersson MN, McKenna DD. 2020. The diversity
588 and evolution of odorant receptors in beetles (Coleoptera). *Insect Mol Biol.* 29:77-91.

589 Mustaparta H, Tømmerås BÅ, Baeckström P, Bakke JM, Ohloff G. 1984. Ipsdienol-specific
590 receptor cells in bark beetles: structure–activity relationships of various analogues and of
591 deuterium-labelled ipsdienol. *J Comp Physiol.* A 154:591-596.

592 Nei M, Niimura Y, Nozawa M. 2008. The evolution of animal chemosensory receptor gene
593 repertoires: roles of chance and necessity. *Nat Rev Genet.* 9(12):951-963.

594 Price MN, Dehal PS, Arkin AP. 2010. FastTree2 - Approximately maximum-likely hood trees
595 for large alignments. *PLoS ONE.* 5(3):e9490.

596 Raffa KF. 2001. Mixed messages across multiple trophic levels: the ecology of bark beetle
597 chemical communication systems. *Chemoecology* 11:49-65.

598 Raffa KF, Andersson MN, Schlyter F. 2016. Host selection by bark beetles: Playing the odds
599 in a high-stakes game. In: Tittiger C, Blomquist GJ, editors. Advances in insect
600 physiology. Academic press, Oxford. p. 1-74.

601 Ramdya P, Benton R. 2010. Evolving olfactory systems on the fly. *Trends Genet.* 26:307–316.

602 Rastogi S, Liberles DA. 2005. Subfunctionalization of duplicated genes as a transition state to
603 neofunctionalization. *BMC Evol Biol.* 5:28.

604 Rudinsky JA, Furniss MM, Kline LN, Schmitz RF. 1972. Attraction and repression of
605 *Dendroctonus pseudotsugae* (Coleoptera: Scolytidae) by three synthetic pheromones in
606 traps in Oregon and Idaho. *Can Entomol.* 104(6):815-822.

607 Saint-Germain M, Buddle CM, Drapeau P. 2007. Primary attraction and random landing in
608 host-selection by wood- feeding insects: a matter of scale? *Agric For Entomol.* 9:227-235.

609 Schiebe C, Hammerbacher A, Birgersson G, Witzell J, Brodelius PE, Gershenzon J, Hansson
610 BS, Krokene P, Schlyter F. 2012. Inducibility of chemical defenses in Norway spruce bark
611 is correlated with unsuccessful mass attacks by the spruce bark beetle. *Oecologia*
612 170(1):183-198.

613 Schiebe C, Unelius CR, Ganji S, Binyameen M, Birgersson G, Schlyter F. 2019. Styrene, (+)-
614 *trans*-(1*R*,4*S*,5*S*)-4-thujanol and oxygenated monoterpenes related to host stress elicit
615 strong electrophysiological responses in the bark beetle *Ips typographus*. *J Chem Ecol.*
616 45:474-489.

617 Schlyter F, Birgersson G, Byers JA, Bakke A. 1992. The aggregation pheromone of *Ips*
618 *duplicatus* and its role in competitive interactions with *I typographus* (Coleoptera:
619 Scolytidae). *Chemoecology* 3:103-112.

620 Schlyter F, Birgersson G, Leufvén A. 1989. Inhibition of attraction to aggregation pheromone
621 by verbenone and ipsenol. *J Chem Ecol.* 15:2263-2277

622 Schlyter F, Birgersson G, Byers JA, Löfqvist J, Bergström G. 1987. Field response of spruce
623 bark beetle, *Ips typographus*, to aggregation pheromone candidates. *J Chem Ecol.* 13:701-
624 716.

625 Seybold S, Huber D, Lee J, Graves AD, Bohlmann J. 2006. Pine monoterpenes and pine bark
626 beetles: a marriage of convenience for defense and chemical communication. *Phytochem*
627 *Rev.* 5:143-178.

628 Tømmerås BÅ. 1985. Specialization of the olfactory receptor cells in the bark beetle *Ips*
629 *typographus* and its predator *Thanasimus formicarius* to bark beetle pheromones and host
630 tree volatiles. *J Comp Physiol.* A 157:335-342.

631 Tømmerås BÅ, Mustaparta H, Gregoire JC. 1984. Receptor cells in *Ips typographus* and
632 *Dendroctonus micans* specific to pheromones of the reciprocal genus. *J Chem Ecol.*
633 10:759-770.

634 Unelius RC, Schiebe C, Bohman B, Andersson MN, Schlyter F. 2014. Non-host volatile blend
635 optimization for forest protection against the European spruce bark beetle, *Ips typographus*.
636 *PLoS ONE.* 9(1):e85381.

637 Wang G, Carey AF, Carlson JR, Zwiebel LJ. 2010. Molecular basis of odor coding in the
638 malaria vector mosquito Anopheles gambiae. *Proc Natl Acad Sci U S A.* 107(9):4418-4423.

639 Wang X, Wang S, Yi J, Li Y, Liu J, Wang J, Xi J. 2020 Three host plant volatiles, hexanal,
640 lauric acid, and tetradecane, are detected by an antenna-biased expressed odorant receptor
641 27 in the dark black chafer *Holotrichia parallela*. *J Agric Food Chem.* 68(28):7316-7323

642 Wyatt TD. 2014. Coming together and keeping apart: aggregation pheromones and host-
643 marking pheromones. In: Pheromones and animal behavior: Chemical signals and
644 signatures 2nd Edition. Cambridge University Press. Cambridge. p.105-112.

645 Yang Z. 1997. PAML: A program package for phylogenetic analysis by maximum likelihood.
646 Comput *Appl Biosci.* 13(5):555-556.

647 Yang Z, Nielsen R. 1998. Synonymous and nonsynonymous rate variation in nuclear genes of
648 mammals. *J Mol Evol.* 46(4):409-418.

649 Yuvaraj JK, Corcoran JA, Andersson MN, Newcomb RD, Anderbrant O, Löfstedt C. 2017.
650 Characterization of odorant receptors from a non-ditrysian moth, *Eriocrania*
651 *semipurpurella* sheds light on the origin of sex pheromone receptors in Lepidoptera. *Mol*
652 *Biol Evol.* 34(11):2733-2746.

653 Yuvaraj JK, Andersson MN, Corcoran JA, Anderbrant O, Löfstedt C. 2018. Functional
654 characterization of odorant receptors from *Lampronia capitella* suggests a non-ditrysian
655 origin of the lepidopteran pheromone receptor clade. *Insect Biochem Mol Biol.* 100:39-47.

656 Yuvaraj JK, Roberts RE, Sonntag Y, Hou X-Q, Grosse-Wilde E, Machara A, Zhang D-D,
657 Hansson BS, Johanson U, Löfstedt C, Andersson MN. 2021. Putative ligand binding sites
658 of two functionally characterized bark beetle odorant receptors. *BMC Biol.* 19:16.

659 Zhang DD, Zhu KY, Wang CZ. 2010. Sequencing and characterization of six cDNAs
660 putatively encoding three pairs of pheromone receptors in two sibling species, *Helicoverpa*
661 *armigera* and *Helicoverpa assulta*. *J Insect Physiol.* 56(6):586-593.

662 Zhang DD, Löfstedt C. 2013. Functional evolution of a multigene family: orthologous and
663 paralogous pheromone receptor genes in the turnip moth, *Agrotis segetum*. *PLoS ONE.*
664 8(10):e77345.

665 Zhang DD, Löfstedt C. 2015. Moth pheromone receptors: gene sequences, function and
666 evolution. *Front Ecol Evol.* 3:105.

667 Zhang DD, Wang HL, Schultze A, Froß H, Francke W, Krieger J, Löfstedt C. 2016. Receptor
668 for detection of a Type II sex pheromone in the winter moth *Operohphtera brumata. Sci*
669 *Rep.* 6:18576.

670 Zhang QH, Schlyter F. 2004. Olfactory recognition and behavioural avoidance of angiosperm
671 non-host volatiles by conifer bark beetles. *Agric For Entomol.* 6:1-19.

672 Zhao T, Krokene P, Björklund N, Långström B, Solheim H, Christiansen E, Borg-Karlson A-
673 K. 2010. The influence of *Ceratocystis polonica* inoculation and methyl jasmonate
674 application on terpene chemistry of Norway spruce, *Picea abies*. *Phytochemistry* 71:1332-
675 1341.

676 Zhao T, Ganji S, Schiebe C, Bohman B, Weinstein P, Krokene P, Borg-Karlson A-K, Unelius
677 CR. 2019. Convergent evolution of semiochemicals across Kingdoms: bark beetles and
678 their fungal symbionts. *ISME J.* 13:1535-1545.

679 Økland B, Bjørnstad ON. 2003. Synchrony and geographical variation of the spruce bark beetle
680 (*Ips typographus*) during a non-epidemic period. *Popul Ecol.* 45:213-219.

681 **Figure legends**

682 **Fig. 1.** (A) Unrooted maximum likelihood phylogenetic tree showing the relationships among
683 select Group 7 (Mitchell et al., 2020) odorant receptors (ORs) from *Ips typographus* ('Ityp';
684 blue) and *Dendroctonus ponderosae* ('Dpon'; red). The tree is based on a MAFFT alignment
685 of amino acid sequences and constructed using FastTree 2.1.11. The clade containing the seven
686 ItypORs is highlighted in yellow and the strong purifying selection ($\omega = 0.0762$) is indicated
687 on the branch. Numbers at nodes are local support values, calculated using the Shimodaira-
688 Hasegawa (SH) test implemented in FastTree (SH values below 0.7 are not shown). (B) The
689 primary ligands and expression levels (transcripts per million; TPM) relative to Orco of the
690 seven *Ips*-specific ORs (data from Yuvaraj et al., 2021). (C)The pair-wise amino acid identity
691 amongst the seven ORs, based on a MAFFT alignment. (D) Chemical structures of the main
692 ligand for each of the seven ItypORs in the clade.

693 **Fig. 2.** Responses of ItypOR23 in oocytes. (A) Representative current traces of oocytes upon
694 successive exposures to 100 μM stimuli. Each compound was applied at the time indicated by
695 the arrowheads for 20 s. Upper and lower traces include different sets of test stimuli. (B)
696 Response profile of ItypOR23 to the full odor panel. Values were normalized based on the
697 average response to the primary ligand of ItypOR23 ($n \geq 4$). (C) Dose-dependent responses of
698 oocytes expressing ItypOR23/Orco to active ligands. Values were normalized based on the
699 average response of ItypOR23 to the most active compound at 100 μM ($n \geq 4$ for each ligand).
700 Error bars indicate the SE.

701 **Fig. 3.** Responses of ItypOR29 in oocytes. (A) Representative current traces of oocytes upon
702 successive exposures to 100 μM stimuli. Each compound was applied at the time indicated by
703 the arrowheads for 20 s. Upper and lower traces include different sets of test stimuli. (B)
704 Response profile of ItypOR29 to the full odor panel. Values were normalized based on the
705 average response to the primary ligand of ItypOR29 ($n \geq 4$). (C) Dose-dependent responses of
706 oocytes expressing ItypOR29/Orco to active ligands. Values were normalized based on the
707 average response of ItypOR29 to the most active compound at 100 μM ($n \geq 4$ for each ligand).
708 Error bars indicate the SE.

709 **Fig. 4.** Responses of ItypOR25 in oocytes. (A) Representative current traces of oocytes upon
710 successive exposures to 100 μM stimuli. Each compound was applied at the time indicated by
711 the arrowheads for 20 s. Upper and lower traces include different sets of test stimuli. (B)
712 Response profile of ItypOR25 to the full odor panel. Values were normalized based on the
713 average response to the primary ligand of ItypOR25 ($n \geq 4$). (C) Dose-dependent responses of

714 oocytes expressing ItypOR25/Orco to active ligands. Values were normalized based on the
715 average response of ItypOR25 to the most active compound at 100 μM (n ≥4 for each ligand).
716 Error bars indicate the SE.

717 **Fig. 5.** Responses of ItypOR27 in oocytes. (A) Representative current traces of oocytes upon
718 successive exposures to 100 μM stimuli. Each compound was applied at the time indicated by
719 the arrowheads for 20 s. Upper and lower traces include different sets of test stimuli. (B)
720 Response profile of ItypOR27 to the full odor panel. Values were normalized based on the
721 average response to the primary ligand of ItypOR27 (n ≥ 4). (C) Dose-dependent responses of
722 oocytes expressing ItypOR27/Orco to active ligands. Values were normalized based on the
723 average response of ItypOR27 to the most active compound at 100 μM (n ≥ 3 for each ligand).
724 Error bars indicate the SE.

725 **Fig. 6.** Responses of ItypOR28 in oocytes. (A) Representative current traces of oocytes upon
726 successive exposures to 100 μM stimuli. Each compound was applied at the time indicated by
727 the arrowheads for 20 s. Upper and lower traces include different sets of test stimuli. (B)
728 Response profile of ItypOR28 to the full odor panel. Values were normalized based on the
729 average response to the primary ligand of ItypOR28 (n ≥ 4). (C) Dose-dependent responses of
730 oocytes expressing ItypOR28/Orco to active ligands. Values were normalized based on the
731 average response of ItypOR28 to the most active compound at 100 μM (n ≥ 4 for each ligand).
732 Error bars indicate the SE.

733 **Table 1.** Comparing *in vitro* responses of odorant receptors (ORs) with OSN responses. Rank
734 order (1 = best compound, 2 = second best, etc.) based on response magnitude (SSR data
735 from Tømmerås, 1985; Andersson et al., 2009; Schiebe et al., 2019; Kandasamy, 2019).
736 Normalized responses for ItypORs in oocytes.

Stimulus[a]	Matching ORs/OSNs							
	1		2		3		4[c]	
	OR23	OSN tMTol	OR25[b]	OSN Δ3	OR27	OSN pC	OR29	OSN Pcn
(+)-*trans*-4-Thujanol	1	1	5	2	2	2	-	-
(–)-Terpinen-4-ol	2	2	-	-	-	-	-	-
(±)-3-Octanol	2	2	5	-	-	-	-	-
(±)-1-Octen-3-ol	-	3	-	-	-	-	-	-
Acetophenone	3	-	5	4	-	-	-	-
(+)-3-Carene	-	-	1	1	-	2	-	-
(+)-*trans*-Verbenol	-	-	2	-	-	-	-	-
Styrene	-	-	6	2	-	-	-	-
1-Hexanol	-	-	3	3	-	-	-	-
p-Cymene	-	-	-	-	1	1	-	-
γ-Terpinene	-	-	-	-	1	1	-	-
α-Pinene	-	-	5	4	-	2	-	-
Lanierone	-	-	4	-	-	-	-	-
α-Isophorone	-	-	4	-	-	-	-	-
(+)-Isopinocamphone	-		6	3	-	-	1	1
(–)-Isopinocamphone	-	-	-	-	-	-	3	3
(+)-Pinocamphone	-	-	-	-	-	-	2	2
(–)-Pinocamphone	-	-	-	-	-	-	3	5
(–)-Pinocarvone	-	-	-	-	-	-	3	3
(±)-Camphor	-	-	6	3	-	-	4	4

737 Repeated number in the same column indicates similar response magnitude.

738 [a)] Only stimuli that were tested on both the OR and the putatively corresponding OSN class
739 are shown.

740 [b)] Additional compounds eliciting minute screening responses in ItypOR25 are not listed for
741 clarity.

742 [c)] Note, apart from (+)-isopinocamphone which stands out as the best ligand, the secondary
743 responses to the structurally related secondary ligands are all very similar; hence, the few
744 discrepancies in compound rank order between the OR and OSNs are minor in terms of
745 sensitivity.
746
747
748
749
750
751
752
753
754

755 **Figure 1**

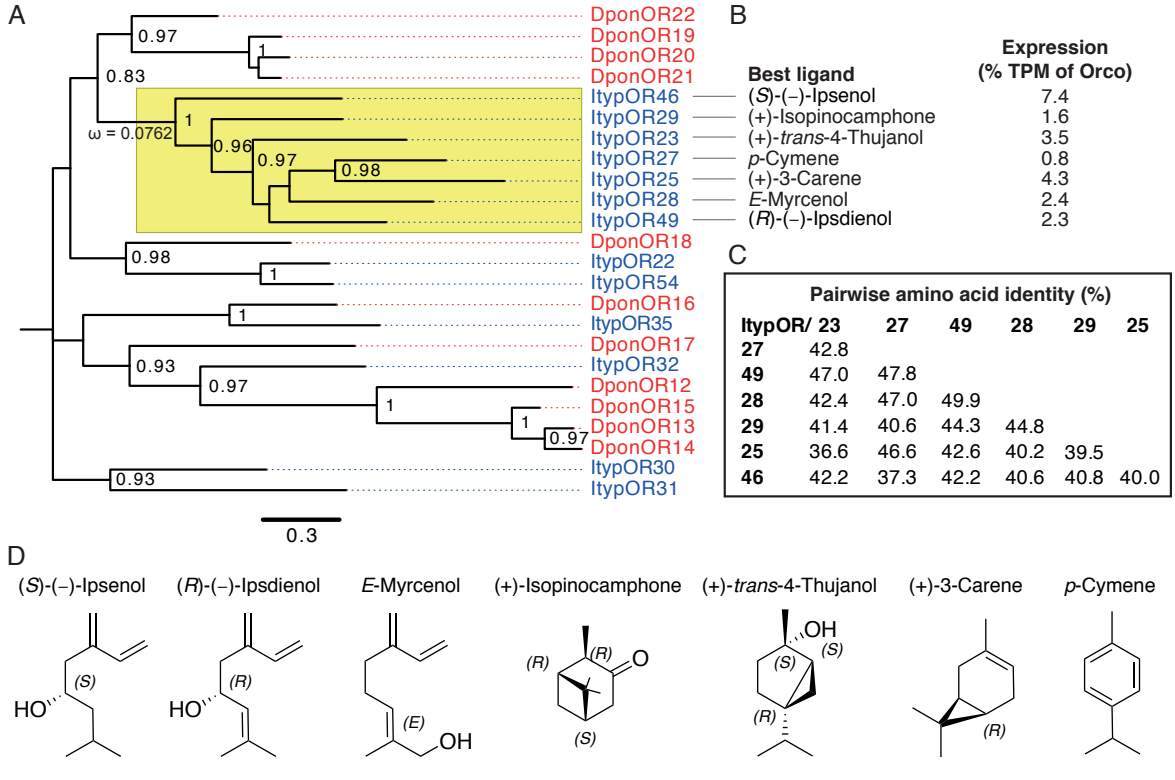

756

757

758 **Figure 2**

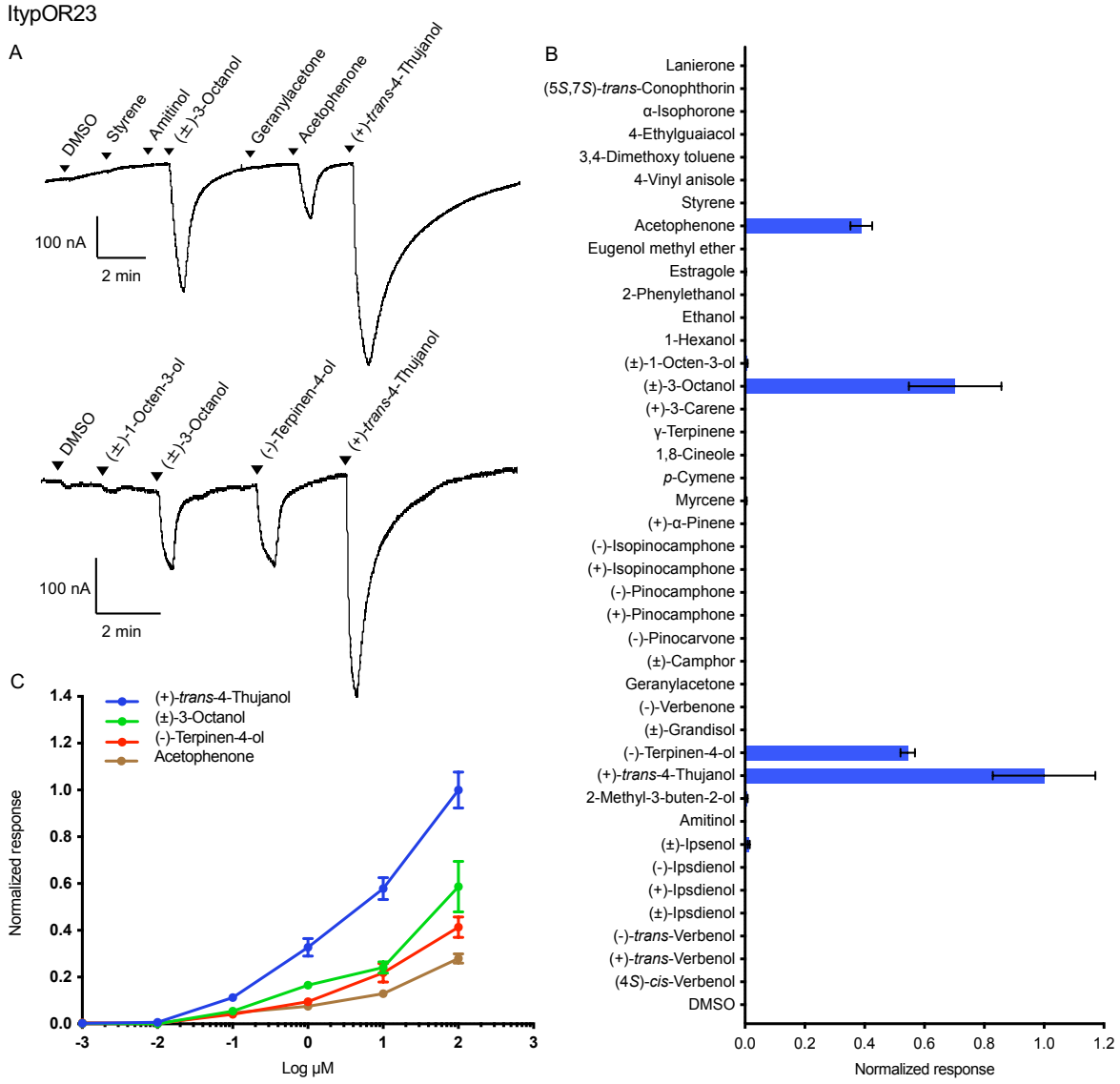

759

760

761 **Figure 3**

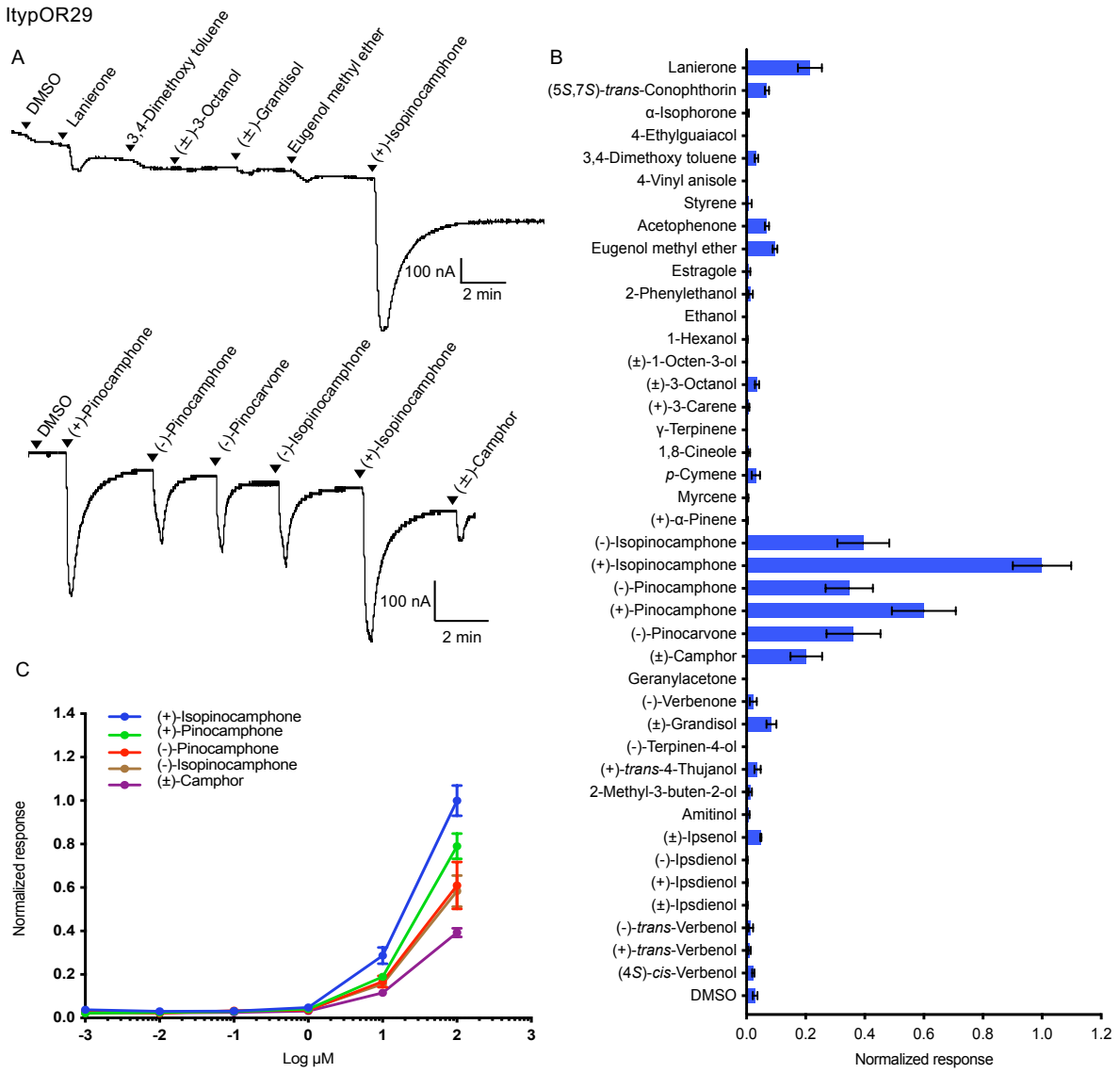

762
763

764 **Figure 4**

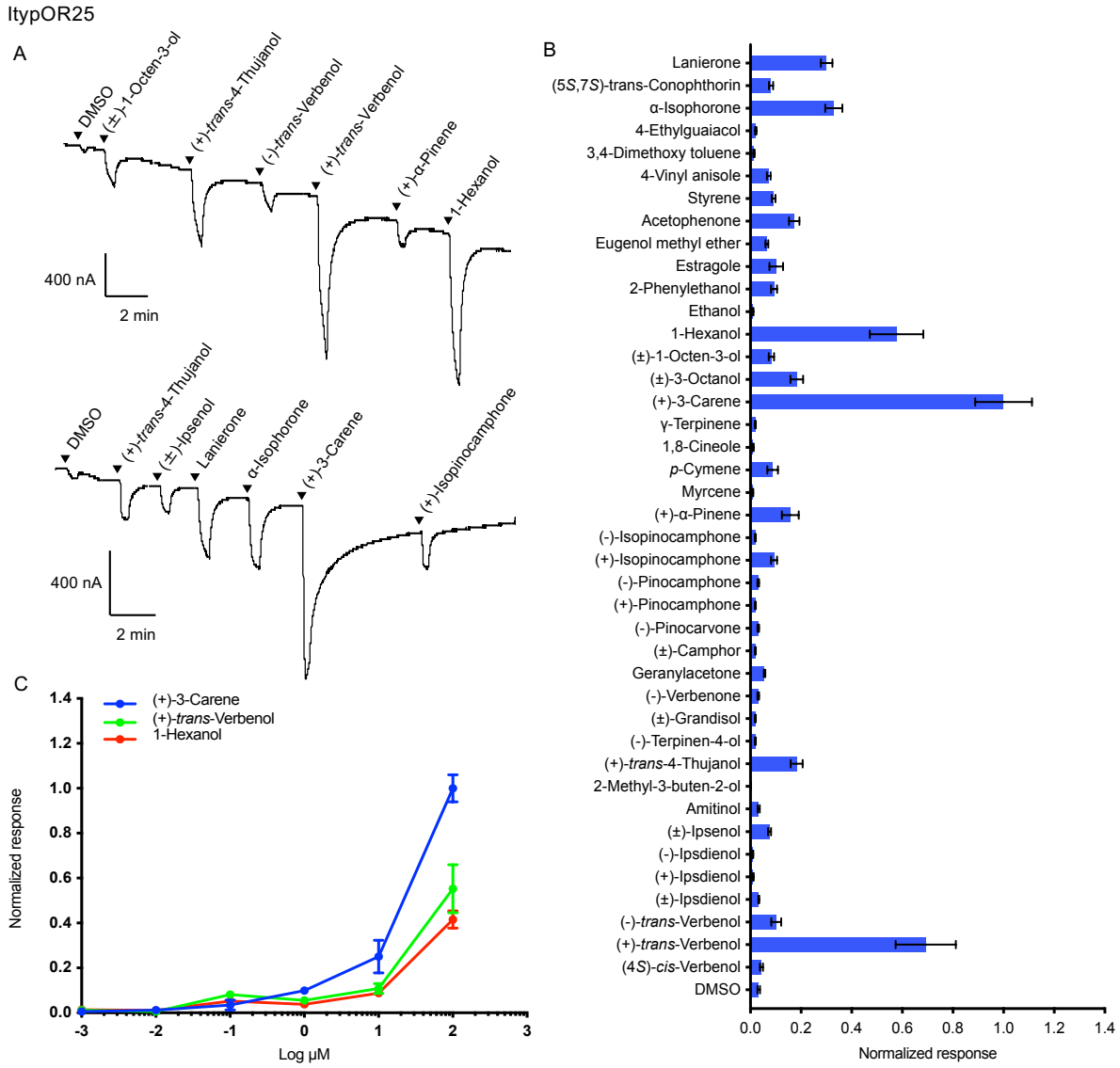

765

766

767 **Figure 5**

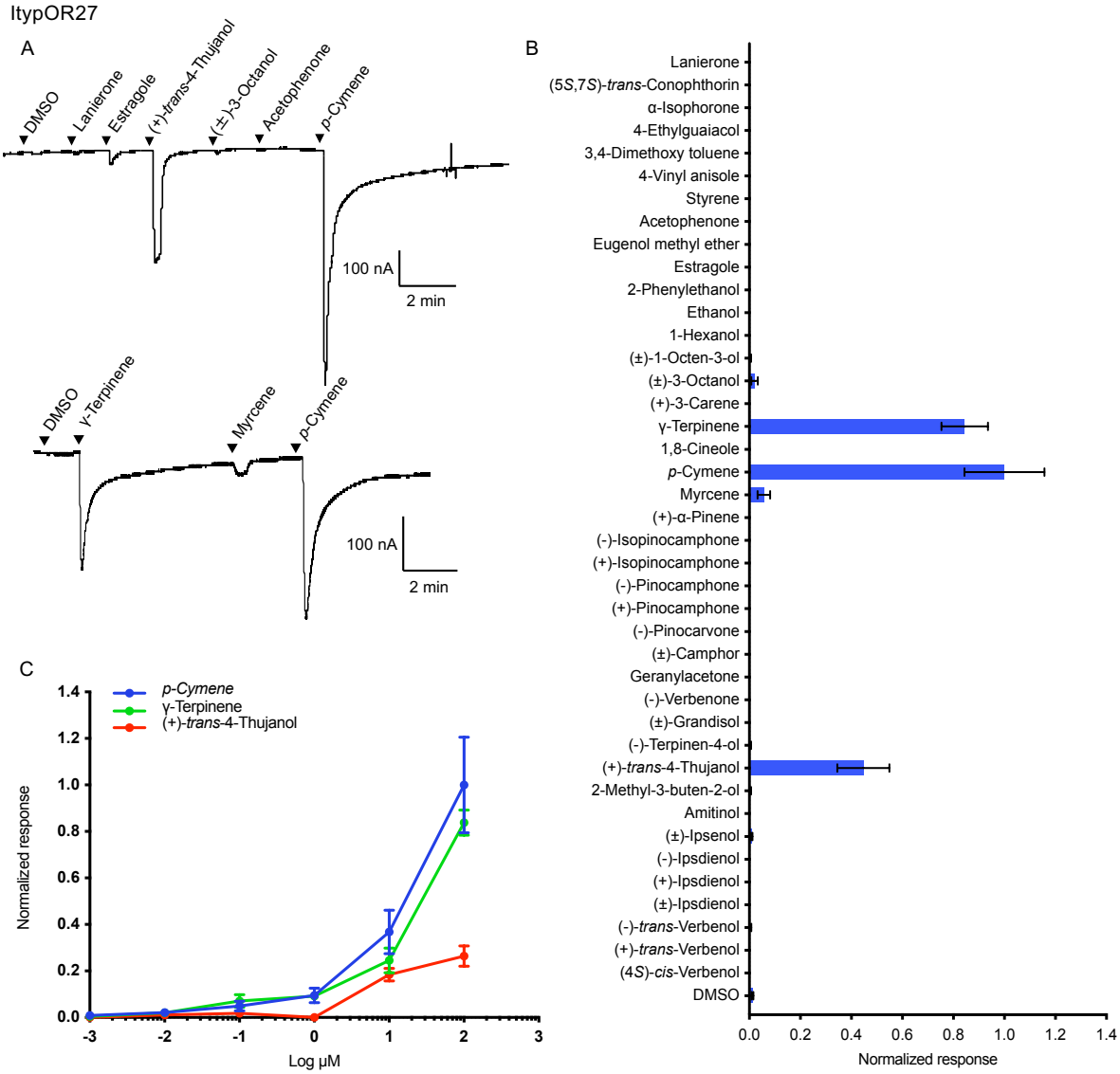

768

769

770 **Figure 6**

ItypOR28

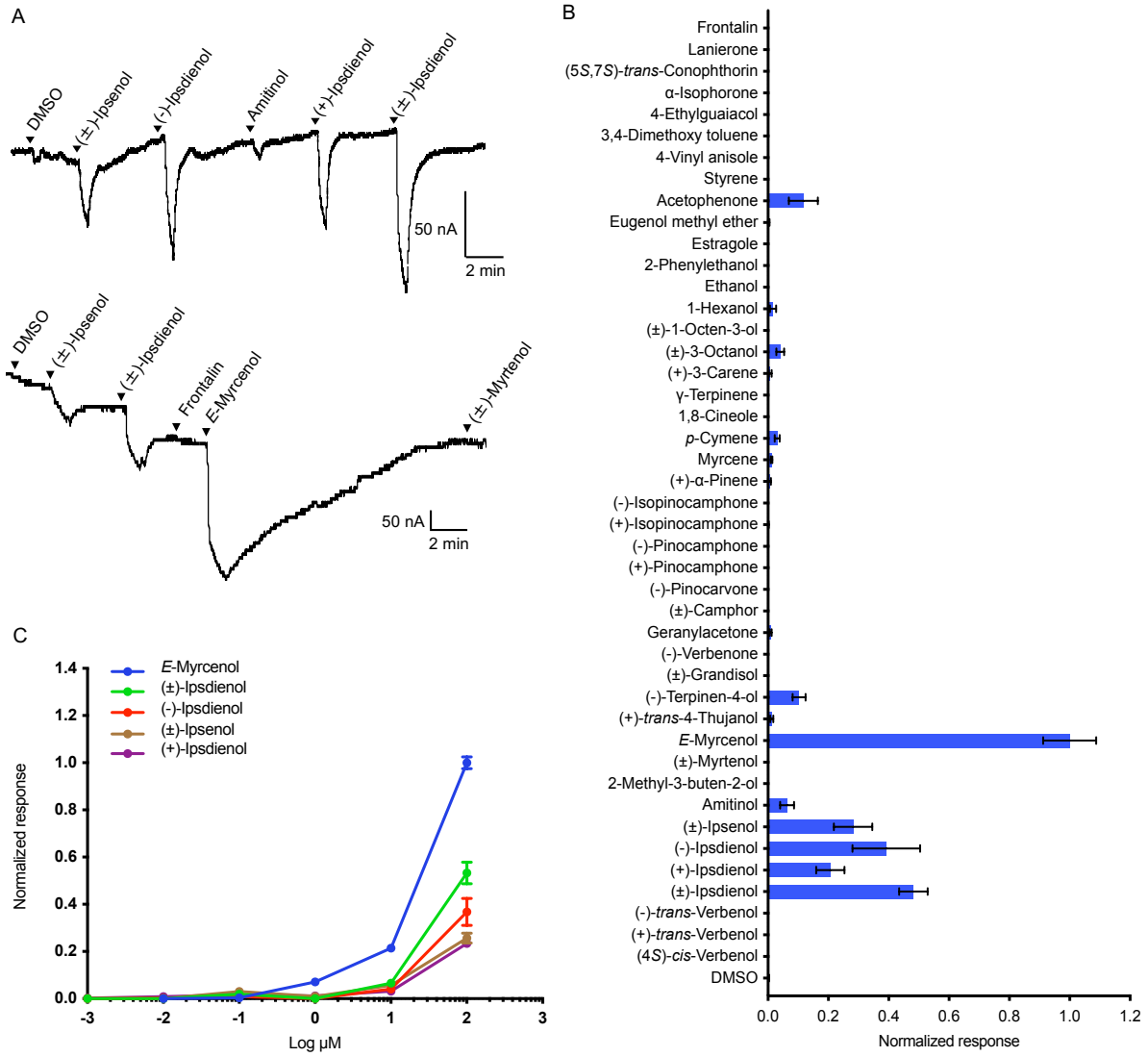

771